Design of novel high strength bainitic steels: Part 2

F. G. Caballero, H. K. D. H. Bhadeshia, K. J. A. Mawella, D. G. Jones, and P. Brown

A combination of thermodynamic, kinetic, and mechanical property models and physical metallurgy principles was used in part 1 of this study to propose a number of alloys which exploit the carbide free bainitic microstructure at its theoretical best. These alloys have been manufactured and the present paper (part 2) reports the results of metallographic characterisation and mechanical tests. The proposed steels are found to have an unprecedented combination of strength and toughness for bainitic microstructures, matching even the maraging steels which are at least thirty times more expensive. The work confirms the alloy design procedures explained in part 1.

MST/4645

At the time the work was carried out Dr Caballero and Professor Bhadeshia were in the Department of Materials Science and Metallurgy, University of Cambridge, Pembroke Street, Cambridge CB2 3QZ, UK (hkdb@cus.cam.ac.uk). Dr Caballero is now at CSIC CNIM, Avda Gregorio del Amo, 8–28040 Madrid, Spain (fgc@cenim.csic.es). Dr Mawella, Mr Jones, and Dr Brown are in the Structural Materials Centre, Defence Evaluation Research Agency, R1079, Building A7, Farnborough, Hants GU14 0LX, UK. *Manuscript received 13 March 2000; accepted 7 August 2000.*

Introduction

In part 1[1] of this two part study, a number of carbide free bainitic steels were proposed for manufacture. The steels were designed on the basis that the fraction of bainitic ferrite obtained by continuous cooling transformation should be high enough to avoid any large and unstable regions of high carbon retained austenite, having only the films of retained austenite to separate the bainite platelets. The steels also had to meet certain hardenability and strength requirements.

The work presented here, in this the second part of the study, is concerned with the microstructural and mechanical property characterisation of the three bainitic steels proposed in part 1. As is shown below, the results are exciting.

Experimental procedure

The actual chemical compositions of the steels studied are given in Table 1. The alloys were prepared as 35 kg vacuum induction melts using high purity base materials. After casting and cropping, the ingots were hot forged down to a thickness of 65 mm. These were then homogenised at 1200°C for 2 days and cut into smaller specimens of 65 mm thickness which were then forged down to 50 mm thickness. These specimens were then held at 900°C for 2 h, removed from the furnace, and immediately hot pressed to a thickness of 25 mm before their temperature fell below 750°C. Finally, they were allowed to cool in air. The particular deformation route used here (Fig. 1) is consistent with a proprietary manufacturing standard.

MICROSTRUCTURAL EXAMINATION OF STEELS

Quantitative X-ray analysis was used to determined the volume fraction of retained austenite. For this purpose, samples were cut from undeformed regions of Charpy specimens. After grinding and final polishing using 0·25 μm diamond paste, the samples were etched to obtain an undeformed surface. They were then step scanned in a Philips PW1730 X-ray diffractometer using unfiltered Cu K_α radiation. The scanning speed (2θ) was 1 deg min^{-1}. The machine was operated at 40 kV and 40 mA. The retained austenite content was calculated from the integrated intensities of (200), (220), and (311) austenite peaks, and those of (002), (112), and (022) planes of ferrite.[2] Using three peaks from each phase avoids biasing the results due to any crystallographic texture in the samples.[3] The carbon concentration in the austenite was estimated by using the lattice parameters of the retained austenite.[4]

Samples for transmission electron microscopy (TEM) were machined down to 3 mm dia. rod. The rods were sliced into discs of 100 μm thickness and subsequently ground down to foils of 50 μm thickness on wet 800 grit silicon carbide paper. These foils were finally electropolished at room temperature, until perforation occurred, using a twin jet electropolisher set at a voltage of 40 V. The electrolyte consisted of 5% perchloric acid, 15% glycerol, and 80% methanol. The foils were examined in a JEOL JEM 200CX transmission electron microscope at an operating voltage of 200 kV.

Optical and scanning electron microscopy (SEM) were used to examine the etched microstructures. Samples were polished in the usual way and etched in 2% nital solution, and examined using a JEOL JXA 820 scanning electron microscope operated at 10–15 kV. The volume fraction of bainite V_B was estimated by a systematic manual point counting procedure on scanning electron micrographs.[5] A grid superimposed on the microstructure provides, after a suitable number of placements, an unbiased statistical estimate of V_B.

DETERMINATION OF MECHANICAL PROPERTIES

Tensile testing was carried out in accordance with BS EN 10 002–1 : 1990 at room temperature on a 100 kN

Table 1 Actual chemical composition of designed alloys, wt-%

Alloy	C	Si	Mn	Cr	Mo	Ni	V
Mn	0·32	1·45	1·97	1·26	0·26	<0·02	0·10
Ni1	0·31	1·51	<0·01	1·44	0·25	3·52	0·10
Ni2	0·30	1·51	<0·01	1·42	0·25	3·53	<0·005

Table 2 Ac_1 and Ac_3 temperatures, °C

Alloy	Ac_1	Ac_3
Mn	807	881
Ni1	759	818
Ni2	775	835

Instron 6025 machine at a crosshead speed of 2 mm min^{-1}. Two specimens were tested for each alloy.

Impact toughness was measured at temperatures between 20 and −120°C using a 300 J Charpy testing machine. Specimens were tested in accordance with BS EN 10 045–1 : 1990. Six specimens were tested at each temperature for every alloy.

Compact tension specimens were used to measure values of plane strain fracture toughness K_{IC} at room temperature for the Ni1 and Ni2 alloys in accordance with BS 7448 : 1991, Part 1. Compact tension/fracture toughness testing was performed on a 100 kN ESH servohydraulic machine. The crosshead speed used was 1 mm min^{-1}.

Vickers hardness testing was carried out using a load of 30 kg and the values presented were averaged over 10 tests.

Fractography was carried on the Charpy impact toughness specimens using a JEOL JXA 820 scanning electron microscope operating at 20 kV.

TEMPERED MICROSTRUCTURES

Austenite formation begins during heating at the Ac_1 temperature and is completed when the Ac_3 temperature is reached. Tempering must be carried out below the Ac_1 temperature to avoid the accidental formation of austenite. The austenite formation temperatures were therefore determined using a Thermecmastor Z thermomechanical simulator. Cylindrical specimens 12 mm in height and 8 mm in diameter were heated at a rate of 10 K s^{-1} to 1000°C and then cooled at 10 K s^{-1}. The formation of austenite during heating was detected by monitoring the fractional change in dilatation with temperature. The Ac_1 and Ac_3 temperatures are given in Table 2. Note that the Ac_1 temperature is ill defined in the present context because the microstructures already contain some retained austenite. The Ac_1 temperature should therefore be interpreted to mean the temperature at which austenite growth begins during heating at the specified rate.

Specimens of the three alloys were tempered at temperatures ranging from 400 to 700°C for 1 h. Samples for TEM were produced as described above.

Results and discussion

CHARACTERISATION OF MICROSTRUCTURE

Experimental data of the designed steel microstructures are given in Table 3. These data and the micrographs shown in Fig. 2 reveal that Ni1 and Ni2 have the desired microstructure consisting of mainly bainitic ferrite and retained austenite. Because of the high carbon content in austenite x_γ for these alloys (Table 3), most of residual austenite present after bainite is formed is retained on cooling to room temperature.

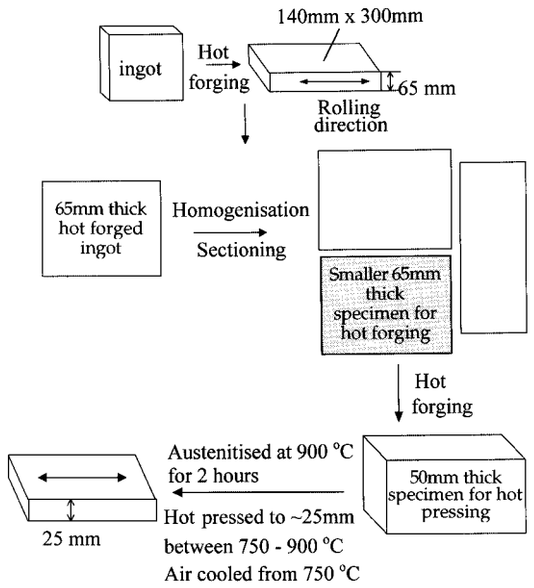

1 Manufacturing route

In the SEM micrographs, martensite regions are relatively unetched, and appear light in colour. The thin interlath films of austenite, however, have been etched away. It is difficult in thin foil TEM experiments to judge whether any martensite has formed as a result of the thinning process or whether it was present in the original microstructure. To cope with this, the specimens were tempered at 200°C for 2 h before making foils. Thus, martensite present in the original specimens would contain carbides, whereas any untempered martensite can be interpreted to be austenite which underwent transformation during the foil preparation process. The observation of tempered microstructures (Fig. 2*c*) showed that the unetched regions in Fig. 2*b* are martensitic. Note that the low temperature (200°C) tempering does not affect bainitic ferrite, since the latter does not contain excess carbon.

Owing to the high volume fraction of bainitic ferrite in Ni1 and Ni2 alloys, 0·62 and 0·81 respectively, the retained austenite was largely present as films between the subunits of bainitic ferrite. Figure 3 shows typical bright field images of carbide free upper bainite in Ni1 and Ni2 with interlath retained austenite films. These films have the typical wavy morphology characteristic of the bainite in high silicon steels (Fig. 3*b*).[6–9]

By contrast, the small amount of bainite in the Mn alloy (Table 3) causes much of the residual austenite to transform to martensite during cooling because of lower carbon enrichment of the austenite (0·55%, Table 3). There is only 10% of the residual austenite retained to room temperature ($V_\gamma = 0{\cdot}07$, Table 3). These results are consistent with the data on instability of residual austenite as function of austenite carbon content illustrated elsewhere.[10]

Table 3 Quantitative data on microstructure and hardness*

Alloy	Volume fraction of bainitic ferrite V_B	Volume fraction of retained austenite V_γ	Volume fraction of martensite $V_{\alpha'}$	C content of austenite x_γ, wt-%	Hardness, HV30
Mn	0·26±0·01	0·07±0·01	0·67±0·02	0·55	597±2
Ni1	0·62±0·05	0·12±0·01	0·26±0·04	0·92	493±5
Ni2	0·81±0·06	0·11±0·01	0·08±0·05	1·03	536±6

*Hardness values are averaged over 10 tests.

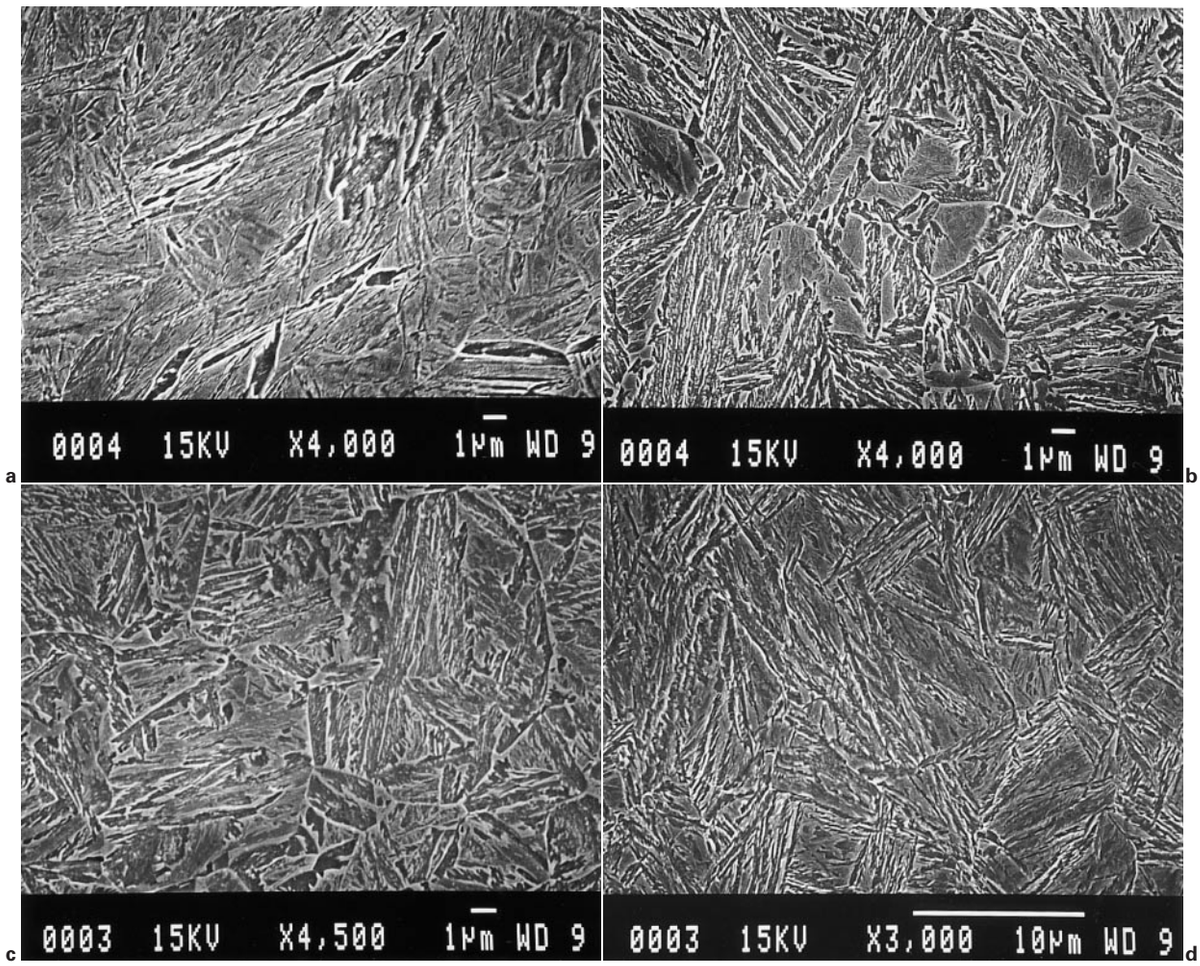

a Mn alloy, as received; *b* Ni1 alloy, as received; *c* Ni1 alloy, as tempered at 200°C for 2 h; *d* Ni2 alloy, as received

2 Microstructures of designed alloys (SEM)

The results of hardness tests are given in Table 4. There is no doubt that the microstructures of Ni1 and Ni2 alloys in the as received condition consist mainly of bainite and retained austenite. Their hardness values are closer to those of microstructures obtained isothermally at 375°C than the respective hardness values of the martensite as determined on water quenching following austenitisation at 1000°C for 15 min. Any difference between the hardness values of as received and isothermally transformed microstructures in Ni1 and Ni2 alloys is due to the different degree of transformation to bainitic ferrite. Not surprisingly, the hardness value for the as received microstructure of Mn alloy (Fig. 2*a*) is similar to that of a fully martensitic sample.

Table 4 Hardness data* of different microstructures of alloys studied

Alloy	Heat treatment	Hardness, HV30
Mn	As received microstructure	597±2
	Water quenched (WQ)	605±5
	350°C for 30 min, WQ	467±7
Ni1	As received microstructure	493±5
	Water quenched	647±8
	375°C for 30 min, WQ	426±4
Ni2	As received microstructure	536±6
	Water quenched	669±7
	375°C for 30 min, WQ	423±9

*Hardness values are averaged over 10 tests.

MECHANICAL PROPERTIES

Tensile strength and ductility

The tensile test results are given in Table 5. Plates of bainitic ferrite were typically 10 μm in length and about 0·2 μm in thickness (Fig. 3). This gives a rather small mean free path for dislocation glide. Thus, the main microstructural contribution to the strength of bainite is from the extremely fine grain size of bainitic ferrite.[11]

It is difficult to separate the effect of retained austenite on strength in these steels from other factors. Qualitatively, austenite can affect the strength in several ways. Residual austenite can transform to martensite during cooling to room temperature, thus increasing the strength as observed in Mn alloy (Tables 3 and 5). On the other hand, retained austenite interlath films can increase the strength by transforming to martensite during testing, similar to the behaviour of TRIP (transformation induced plasticity) steels.

The low yield/ultimate tensile strength ratios (YS/UTS) in Table 5 are due to the presence of austenite and the generally large dislocation density in the microstructure.[12] Consequently, retained austenite increases the strain hardening rate of the steel. Similarly, tensile elongation is controlled by the volume fraction of retained austenite.[13] Retained austenite is a ductile phase compared to the bainitic ferrite and would be expected to enhance ductility in as far as the austenite is homogeneously distributed along plate boundaries (film austenite). However, isolated pools of austenite (blocky austenite) would influence unfavour-

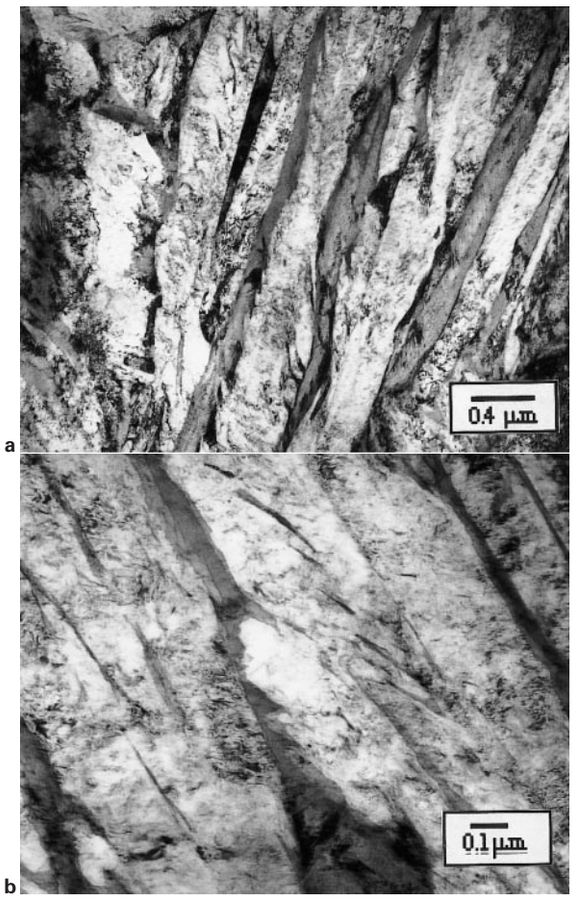

a Ni1 alloy; *b* Ni2 alloy

3 Typical bright field images of microstructures formed by bainitic ferrite and films of retained austenite

ably both elongation and UTS. From Table 5, it is apparent that the steels present a combination of high strength and good ductility. Moreover, tensile properties are much higher than those required for defence applications, i.e. proof strength (YS) 1000 MPa, tensile strength (UTS) 1100 MPa, minimum ductility of 12% elongation, and 50% reduction of area.

Impact toughness

The Charpy impact test results are given in Table 6 for all the alloys. The levels required of impact toughness for defence applications have also been well achieved (i.e. Charpy V notch impact energy of 40 J at −40°C). A considerable improvement in toughness is obtained when the volume fraction of bainite increases in the microstructure. This improvement occurs despite the fact that the strength of the microstructures involved remains almost unchanged (Table 5). From the data in Table 3, it is evident that the volume fraction of bainite and thus the carbon content of the retained austenite explains the improvement in toughness observed in Ni1 and Ni2 alloys as compared

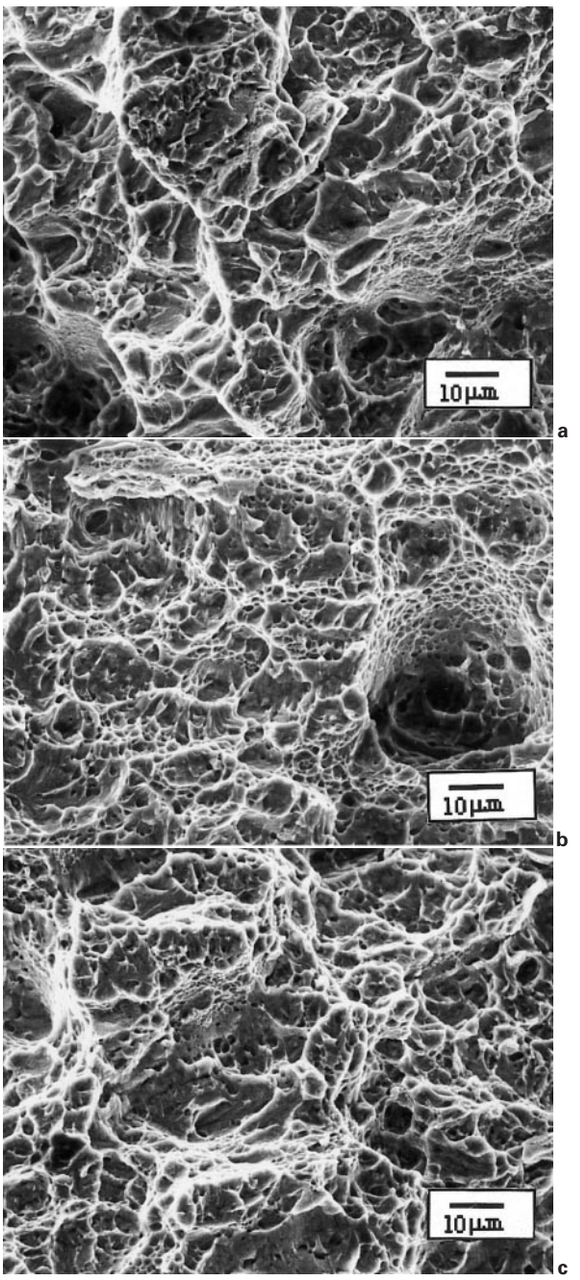

a Mn alloy; *b* Ni1 alloy; *c* Ni2 alloy

4 Fracture surfaces of Charpy impact specimens tested at room temperature (SEM)

with the Mn alloy. The results are consistent with the enhancement of toughness expected when the amount of blocky austenite and martensite are reduced and, in general, when the stability of residual austenite is increased. Figure 4 shows the fracture surfaces of the Charpy impact specimens tested at room temperature. The alloys Ni1 and Ni2 show ductile dimpled fracture surfaces, whereas the Mn alloy,

Table 5 Tensile and fracture toughness properties

Alloy	YS, MPa	UTS, MPa	El., %	RA, %	K_{max}, MPa $m^{1/2}$	J_{max}, MPa m	K_{Jmax}, MPa $m^{1/2}$
Mn	1167	1790	13	44	…	…	…
Ni1	1150	1725	14	55	125	0·114	160
Ni2	1100	1625	14	59	128	0·134	174

YS yield stress; UTS ultimate tensile strength; El. elongation; RA reduction of area.
K_{max} stress intensity factor at maximum load; J_{max} *J*-integral at maximum load; K_{Jmax} stress intensity values calculated from J_{max} values.

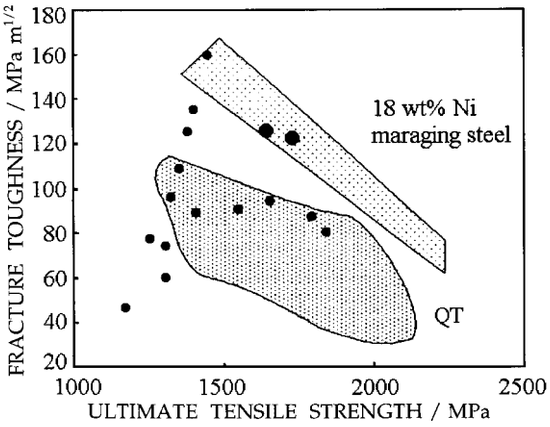

5 Properties of mixed microstructures of bainitic ferrite and austenite versus those of quenched and tempered (QT) low alloy martensitic alloys and maraging steels

which contains a large amount of martensite, has many of the features of quasicleavage with isolated patches of ductile fracture.

Fracture toughness

A compact tension specimen design was used with thickness $B=23{\cdot}1$ mm, width $W=46{\cdot}5$ mm, and crack length ($a=24{\cdot}5$ mm) to width ratio $a/W=0{\cdot}5$. With the measured yield stress of 1100 MPa, this would give a plane strain K_{IC} measurement capacity of ~ 300 MPa m$^{1/2}$. In the event, none of the specimens failed at sufficiently low load to satisfy the K_{IC} validity requirement.

The specimens showed a fairly significant non-linearity before maximum load. This disqualified the use of K_Q as a K_{IC} measurement. The values quoted in Table 5 are for the stress intensity at maximum load K_{max}. All the tests failed by microvoid coalescence with no sign of cleavage. Tearing was stable at maximum load under displacement control. Taking account of the non-linearity in the trace up to maximum load gives the J-integral at maximum load J_{max} and the stress intensity K_{Jmax} calculated from J_{max} values listed in Table 5.

Although the fracture toughness results obtained cannot be considered valid, the results are promising in that the steels tested are so tough that larger specimens would be required to measure K_{IC}. Toughness values of nearly 130 MPa m$^{1/2}$ have been obtained for strength in the range of 1600–1700 MPa. The good fracture toughness obtained in these alloys is attributed to the presence of thin films of thermally and mechanically stable interlath retained austenite. The role of retained austenite is to refine the effective fracture grain size and to blunt a propagating crack.[14]

Figure 5 shows properties of mixed microstructures of bainitic ferrite and austenite versus those of quenched and tempered low alloy martensitic alloys and maraging steels.[8] Small points in the graph refer to previous work,[6–8,10,14]

Table 6 Charpy impact test results*

Alloy	Test temp., °C	Impact energy, J
Mn	20	34±1
	−40	31±1
Ni1	20	58±2
	−40	46±1
	−120	34±2
Ni2	20	50±3
	−40	43±1
	−120	25±3

*Each value is a mean of six tests.

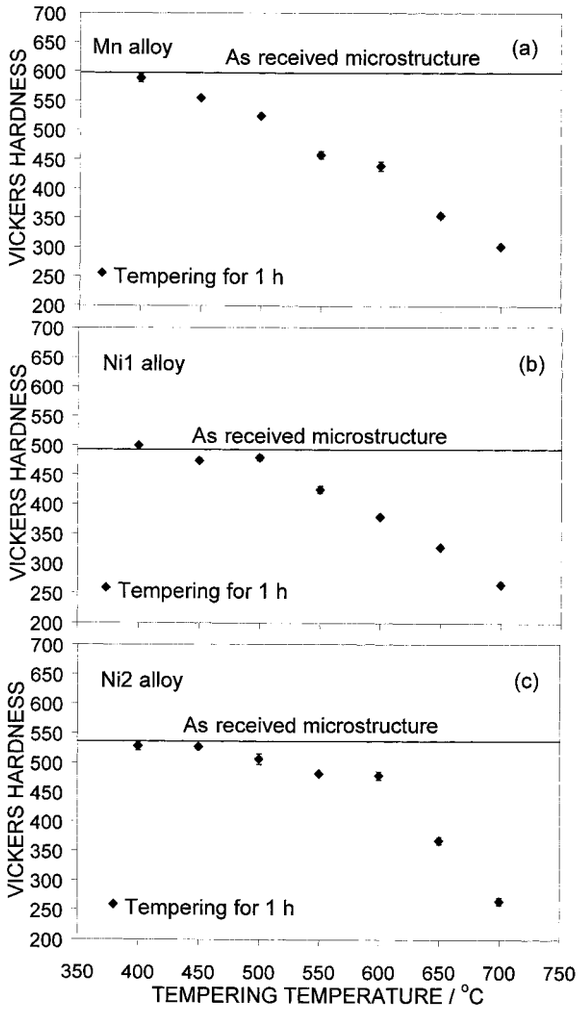

a Mn alloy; *b* Ni1 alloy; *c* Ni2 alloy

6 Plot of hardness values as function of tempering temperature

whereas the two large points correspond to experimental data given in Table 5. The alloys designed theoretically in this work and produced by commercial continuous cooling present the highest strength–toughness combinations recorded to date for bainitic steels. These alloys show mechanical properties superior to those of the quenched and tempered low alloy martensitic alloys and match the critical properties of maraging steels, which are at least thirty times more expensive.

CHARACTERISATION OF TEMPERED MICROSTRUCTURES

Figure 6 shows plots of hardness values as a function of tempering temperature for the three alloys studied. Tempering the designed microstructures of Ni1 and Ni2 steels at temperatures lower than 550°C for 1 h did not result in any significant loss of hardness. However, tempering at 450°C for 1 h the as received microstructure of the Mn alloy led to a drop in the hardness value from 597 to 555 HV30. Since the Mn alloy contains predominantly martensite ($V_{\alpha'}=0{\cdot}67$, Table 3) tempering at 400°C for 1 h is expected to lead to the precipitation of any excess carbon. This is confirmed by Fig. 7*a* which shows discrete carbide particles precipitated inside a martensite plate in the Mn alloy. The retained austenite was still intact with no significant signs of recovery in the bainitic ferrite.

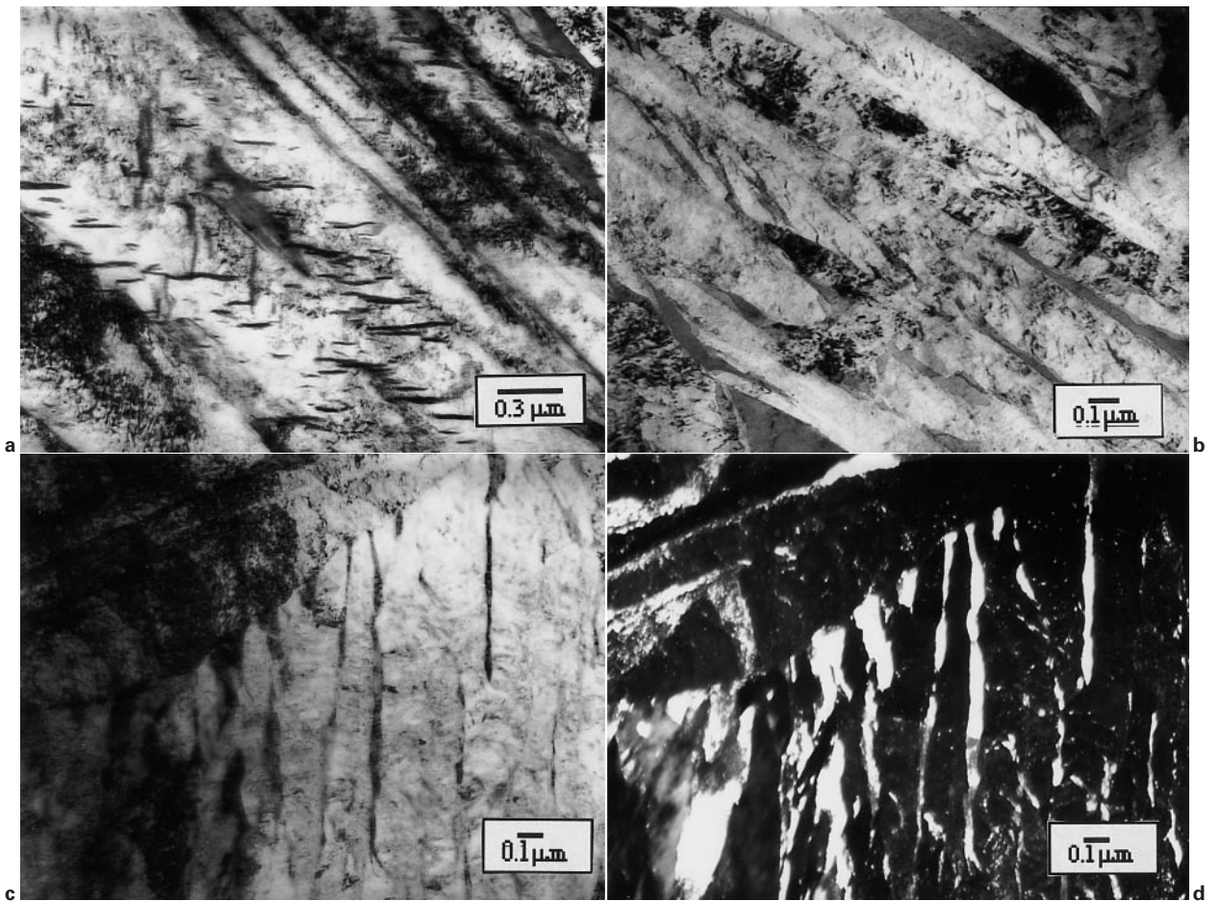

a discrete carbide particles precipitate inside a martensite plate in Mn alloy; *b* no signs of recovery occur in bainitic microstructure of Ni1 alloy; *c* bright field and *d* dark field images reveal that retained austenite is still intact in Ni2 alloy

7 Microstructures obtained by tempering at 400°C for 1 h (TEM)

Bright field images of Ni1 and Ni2 alloy microstructures obtained by tempering at 400°C for 1 h are shown in Fig. 7*b* and *c*. Comparing the tempered microstructures with those of the as received conditions (Fig. 3), it is clear that the tempering at 400°C did not result in any recovery in the bainitic ferrite (Fig. 7*b*) or in the diffusional decomposition of high carbon retained austenite (Fig. 7*c* and *d*).

Conclusions

It has been demonstrated experimentally that models based on phase transformation theory can be applied successfully to the design of high strength–high toughness steels. These alloys, designed to ensure that the hardenability of the steel is sufficient for industrial production, have achieved the highest strength and toughness combinations to date for bainitic steels, at a cost thirty times less than that of maraging steels. It has been found that the two Ni steels also show an important resistance to tempering. These steels have been tempered at temperatures ranging from 400 to 700°C for 1 h and no significant changes in hardness were detected in the microstructure at tempering temperatures lower than 550°C.

Acknowledgements

This work was carried out as part of Technology Group 4 (Materials and Structures) of the MoD Corporate Research Programme. The authors would like to thank Professor A. Windle for the provision of laboratory facilities at the University of Cambridge.

References

1. F. G. CABALLERO, H. K. D. H. BHADESHIA, K. J. A. MAWELLA, D. G. JONES, and P. BROWN: *Mater. Sci. Technol.*, 2001, **17**, 512–516.
2. J. DURNIN and K. A. RIDAL: *J. Iron Steel Inst.*, 1968, **206**, 60.
3. M. J. DICKSON: *J. Appl. Crystallogr.*, 1969, **2**, 176–180.
4. D. J. DYSON and B. HOLMES: *J. Iron Steel Inst.*, 1970, **208**, 469.
5. G. F. VANDER VOORT: 'Metallography: principles and practice', 427; 1984, New York, McGraw-Hill.
6. V. T. T. MIIHKINEN and D. V. EDMONDS: *Mater. Sci. Technol.*, 1987, **3**, 422–431.
7. V. T. T. MIIHKINEN and D. V. EDMONDS: *Mater. Sci. Technol.*, 1987, **3**, 432–440.
8. V. T. T. MIIHKINEN and D. V. EDMONDS: *Mater. Sci. Technol.*, 1987, **3**, 441–449.
9. L. C. CHANG: *Metall. Trans. A*, 1999, **30A**, 909–916.
10. H. K. D. H. BHADESHIA and D. V. EDMONDS: *Met. Sci.*, 1983, **17**, 411–419.
11. K. J. IRVINE, F. B. PICKERING, W. C. HESELWOOD, and M. J. ATKINS: *J. Iron Steel Inst.*, 1957, **195**, 54–67.
12. A. P. COLDREN, R. L. CRYDERMAN, and M. SEMCHYSHEN: 'Steel strengthening mechanisms', 17; 1969, Ann Arbor, MI, Climax Molybdenum.
13. B. P. J. SANDVIK and H. P. NEVALAINEN: *Met. Technol.*, 1981, **15**, 213–220.
14. H. K. D. H. BHADESHIA and D. V. EDMONDS: *Met. Sci.*, 1983, **17**, 420–425.